Aβ_{1-28} Fragment of the Amyloid Peptide Predominantly Adopts a Polyproline II Conformation in an Acidic Solution[†]

Fatma Eker,[‡] Kai Griebenow,[§] and Reinhard Schweitzer-Stenner*,[||]

Departments of Chemistry and Biology, University of Puerto Rico, Río Piedras Campus, P.O. Box 23346, San Juan PR00931, Puerto Rico, and Department of Chemistry, Drexel University, Philadelphia, Pennsylvania 19104

Received March 8, 2004; Revised Manuscript Received April 8, 2004

ABSTRACT: To structurally characterize the nonaggregated state of the amyloid β peptide, which assembles into the hallmark fibrils of Alzheimer disease, we investigated the conformation of the N-terminal extracellular peptide fragment Aβ_{1-28} in D_2O at acidic pD by utilizing combined FTIR and isotropic and anisotropic Raman spectra measured between 1550 and 1750 cm^{-1}. Peptide aggregation is avoided under the conditions chosen. The amide I′ band was found to exhibit a significant noncoincidence effect in that the first moment of the anisotropic Raman and of the IR band profile appears red-shifted from that of the isotropic Raman scattering. A simulation based on a coupled oscillator model involving all 27 amide I′ modes of the peptide reveals that the peptide adopts a predominantly polyproline II conformation. Our results are inconsistent with the notion that the monomeric form of Aβ_{1-28} is a totally disordered, random-coil structure. Generally, they underscore the notion that polyproline II is a characteristic motif of the unfolded state of proteins and peptides.

The main component of plaques found in human patients suffering from Alzheimer's disease is a small peptide, β amyloid (Aβ)[1], comprised of 39−43 amino acids derived from the amyloid Aβ precursor protein (APP) by proteolytic cleavage (*1*). APP is a membrane glycoprotein that exists in various isoforms with a consensus length of 694 amino acids (*1*, 2, 3). The extracellular Aβ(1−42) peptide contains the amino acids 597−638 of the consensus APP sequence (*4*). Several studies have established that the aggregation of Aβ peptides is a prerequisite for the pathogenesis of Alzheimer's disease (*5*). Because of its extreme insolubility and high propensity to aggregate, only a few attempts have been made to identify the solution conformation of the full-length β peptide (*6*, 7). It is generally thought that Aβ_{1-43} and its major fragments are unstructured in an aqueous solution in absence of membrane mimetic and helix-forming reagents (*7*, *8*). This notion was recently challenged by Jarvet et al., whose CD and NMR spectra of Aβ_{12-28} were interpreted as indicating that a substantial fraction of the peptide adopts a polyproline II (PPII) conformation at room temperature (*9*). However, similar CD spectra of a β_{1-40} dimer−trimer mixture and of shorter, monomeric fragments were interpreted by others as reflecting an "irregular" structure (*10*). A final assessment of this issue is of utmost importance for the understanding of the initial phase of Aβ aggregation.

The PPII helix exhibits a nearly perfect 3-fold rotational symmetry for its canonical conformation with (ϕ, ψ) = (−78°, 146°). Its relevance for the initial phase of the amyloid plaque formation of various proteins has recently been reported on the basis of Raman Optical Activity (ROA) measurements. For human lysozyme, Blanch et al. showed that its partially unfolded state exhibits a significant PPII fraction and practically no β-sheet contents (*11*). The respective protein conformation is assignable to a prefibrillar intermediate from which the protein forms amyloid fibrils. Moreover, the brain proteins α synuclein and τ, which were generally considered as being naturally disordered, exhibit a significant PPII content (*12*). Both proteins have a propensity for fibril formation. It was therefore hypothesized that PPII might be a "killer conformation" in the development of neurodegenerative diseases (*11*). However, as pointed out by Syme et al. (*12*), interpeptide association also requires specific residue properties such as a low net charge and high net hydrophibicity as demonstrated by recent experiments of Dobson et al. (*13*).

In this paper, we present a structural analysis of monomeric Aβ_{1-28} in an aqueous solution based on a novel analysis of the amide I′ band profile of its IR and Raman spectra. The conformational flexibility of the β peptide reflects, to a major extent, the conformational propensities of the residues 1−28 (*14*). The hydrophobic Aβ_{29-42} segment has a high intrinsic propensity for a β-strand conformation. Aβ_{1-28} is still capable of forming amyloid-like fibrils in vitro, which morphologically resemble fibrils of natural amyloid in vivo (*15*, 16), even though they lack the toxicity of the latter. This plaque incompetent fragment serves as a suitable model system for elucidating the structure of the nonaggregated amyloid

[†] Financial support was provided from the NIH−COBRE II Grant for the Center for Research in Protein Structure, Function, and Dynamics (P20 RR16439-01) and from the Fondos Institucionales para la Investigación of the University of Puerto Rico (20-02-2-78-514).

* To whom correspondence should be addressed. Telephone: (215) 895-2268. Fax: (215) 895-1265. E-mail: rschweitzer-stenner@drexel.edu.

[‡] Department of Biology, University of Puerto Rico.

[§] Department of Chemistry, University of Puerto Rico.

[||] Drexel University.

[1] Abbreviations: FTIR, Fourier transform infrared spectroscopy; ECD, electronic circular dichroism, Aβ, Amyloid β peptide; PPII, Polyproline II helix.

10.1021/bi049542+ CCC: $27.50
Published on Web 05/13/2004

peptide, because it contains key structural features that are important in mediating amyloid fibrillogenesis by electrostatic interactions (*17*). Earlier studies reported a monomeric random-coil conformation at pH < 4 (*8*). Our present analysis, however, strongly indicates that the structure of Aβ_{1-28} can be described as a mixture of local PPII and β-strand conformations.

THEORETICAL BACKGROUND

In this paper, we measured and simulated IR and isotropic and anisotropic Raman spectra of Aβ_{1-28} to determine its predominant conformation. Here, we solely outline the basic principles of the applied theory, which with respect to underlying concepts is just an extension of what is described in detail in ref *18*. A more detailed version will be published separately.

As described in earlier studies (*18*, 19, 20), our approach is based on the excitonic character of the amide I modes of polypeptides, which results from through-bond and transition dipole coupling (*21*). As shown by Choi et al. (*22*) this can be accounted for by a coupled oscillator model, which describes excitonic coupling within a basis set of the vibrational states of local vibrations. Hence, the Schrödinger equation can be written as

$$(\hat{H}_0 + \hat{H}^{\text{ext}})|\chi'\rangle = E|\chi'\rangle \tag{1}$$

where $|\chi'\rangle$ is the state vector comprising the 27 excitonic amide I states of Aβ_{1-28}, $\hat{H}_0$ is the Hamiltonian of the uncoupled local modes, $\hat{H}^{\text{ext}}$ accounts for the excitonic coupling between the modes, and E represents a set of excitonic eigenenergies. As shown by recent ab initio calculations, only nearest-neighbor and second-neighbor coupling have to be taken into account (*21*, *22*). Therefore, we assume that $H^{\text{ext}}_{ij} = \Delta_{ij}$ for $j = i \pm 1$, $i \pm 2$, while all other matrix elements are zero ($i, j = 1, 2, 3, ..., 2$).

The Raman tensors of the excitonic states are written as a linear combination of the local mode tensors

$$\hat{\alpha}'_i = \sum_{j=1}^{27} a_{ij}\hat{\alpha}_j \tag{2}$$

where the coefficients a_{ij} are obtained from the solution of eq 1. In the present context, we assumed identical Raman tensors for the local modes written as (*23*)

$$\hat{\alpha} = \begin{pmatrix} a^* & c^* & 0 \\ c^* & 1 & 0 \\ 0 & 0 & d^* \end{pmatrix} \tag{3}$$

where $\alpha_{yy} \equiv 1$ and the elements a^*, c^*, and d^* are thus expressed in units of a_{yy}. Equation 1 describes the Raman tensor in the earlier described molecular frame (*18*, *19*). The elements c^* and d^* are linearly dependent. The use of eq 2 requires that all Raman tensors be transformed into a common reference system. In our case, we select a coordinate system associated with the C-terminal peptide group. Details are described in earlier papers (*18*, 23). Thus, the obtained $\hat{\alpha}_i$ can be used to calculate the isotropic and anisotropic Raman intensity

$$\beta'^{\,2}_{s,i} = \frac{1}{9}(Tr\ \hat{\alpha}'_i)^2$$

$$\gamma'^{\,2}_{\text{aniso},i} = \frac{1}{2}2[(\alpha'_{xx,i} - \alpha'_{yy,i})^2 + (\alpha'_{yy,i} - \alpha'_{zz,i})^2 + (\alpha'_{zz,i} - \alpha'_{xx,i})^2] + \frac{3}{4}[(\alpha'_{xy,i} + \alpha'_{yx,i})^2 + (\alpha'_{yz,i} + \alpha'_{zy,i})^2 + (\alpha'_{zx,i} + \alpha'_{xz,i})^2] \tag{4}$$

The respective depolarization ratio is written as

$$\rho_i = \frac{3\gamma^2_{\text{aniso},i}}{45\beta^2_{s,i} + 4\gamma^2_{\text{aniso},i}} \tag{5}$$

The IR-intensity profile is calculated correspondingly. The local vector of the transition dipole moment of the jth peptide group is written as

$$\vec{\mu}_j = \begin{pmatrix} \mu_{0j}\cos\vartheta \\ \mu_{0j}\sin\vartheta \\ 0 \end{pmatrix} \tag{6}$$

where ϑ is the orientational angle of $\vec{\mu}_j$ in the x,y plane of the local reference system (*18*). After the local dipole vectors have been transformed into a common reference system (of the C-terminal peptide), the transition dipole moment of the ith excitonic mode can be calculated by utilizing

$$\vec{\mu}_i = \sum_{j=1}^{27} a_{ij}\vec{\mu}_j \tag{7}$$

MATERIALS AND METHODS

Materials. Aβ_{1-28} was obtained from Ana Spec, Inc. The commercial peptides usually contain a small amount of trifluoroacetic acid (TFA) used in HPLC purification, which gives rise to a band at ~1674 cm^{-1} that contaminates the amide I′ region, particularly of the IR spectrum. To remove the residual TFA, the peptide was dialyzed extensively at pH 1.0 by using Spectra/Por Cellulose Ester Float A Lyzer dialysis membranes (M_w cut off of 500). The peptide was directly dissolved in D_2O solution. The corresponding concentration was 3 mM. The pD was adjusted by adding small aliquots of NaOD or DCl. Electrode readings were corrected for the deuterium effects (*24*). The success of the purification step was confirmed by the absence of the very intense IR band at 1674 cm^{-1} and of a weaker, but clearly identifiable, 1610 cm^{-1} band in the isotropic Raman spectrum (*25*).

Methods: Spectroscopies. We used the same equipment and experimental set ups described in earlier publications (*20*). The Raman spectra were obtained with the 514-nm (400 mW) excitation from a Lexel 95 argon ion laser. The vibrational circular dichroism instrumental description is the same as the previous papers (*20*).

Spectral Analysis. To reduce the noise of the Raman spectra caused by a significant fluorescence background, we carried out some smoothing by averaging a set of nine spectra, which were created by shifting the original spectrum

by ±0.5, 1, 1.5, and 2 cm^{-1}. These shifts are negligible compared with the apparent spectral bandwidth, and the averaging has therefore a limited affect on the overall band profiles. All IR and Raman spectra were analyzed using MULTIFIT (*26*). They were normalized to the internal standard, i.e., the D_2O band at 1207 cm^{-1}. Our commonly used internal standard, the 934 cm^{-1} band of the ClO_4^- ion, could not be employed, because the perchlorate ion caused substantial aggregation of Aβ_{1-28}. To eliminate solvent contributions, we measured the solvent reference spectra for both polarizations, which were then subtracted from the corresponding peptide spectra. The intensities of the normalized polarized Raman bands were derived from their band areas. These and the corresponding IR spectrum were self-consistently analyzed in that they were fitted with a set of identical frequencies, half-widths, and band profiles. The isotropic and anisotropic Raman intensities and the depolarization ratios ρ were calculated as

$$I_{\text{iso}} = I_x - \frac{4}{3} I_y$$

$$I_{\text{ansio}} = I_y$$

$$\rho = \frac{I_x}{I_y} \tag{8}$$

It should be mentioned that in principle I_{aniso} should be written as $2.33I_y$. As discussed in our earlier papers (*19*), we prefer to identify it with I_y in the depicted figures so that the polarization properties of different lines can be better inferred.

RESULTS AND DISCUSSION

Figure 1 depicts the FTIR and isotropic and anisotropic Raman spectra of Aβ_{1-28} between 1550 and 1650 cm^{-1}. The amide I′ region can heuristically be decomposed into two Gaussian bands at 1647 (AI′$_1$) and 1675 cm^{-1} (AI′$_2$) with half-widths of 38 and 35 cm^{-1} and depolarization ratios of $\rho_1 = 0.26$ and $\rho_2 = 0.14$, respectively. The respective intensity ratios, AI′$_1$/AI′$_2$, are $R_{\text{IR}} = 3.0$, $R_{\text{iso}} = 0.55$, and $R_{\text{aniso}} = 1.3$. Qualitatively, the spectra can be interpreted by assuming that only 2 of the 27 excitonic amide modes contribute significantly to the observed band profiles (*21*). One of them can be described as the in-phase combination of the local modes (*A* mode). The other one is a 2-fold degenerated E_1 mode and involves out-of-phase combinations of adjacent vibrations. In principle, this simple model is only suitable for infinite helices, but it provides some principal guidance for the interpretation of spectra of even very short peptides (*21*). On the basis of their depolarization ratios, we assign AI′$_1$ to E_1 and AI′$_2$ to *A*. Our experimental data suggest that Aβ_{1-28} adopts an extended conformation assignable to the upper left square of the Ramachandran plot, for which Torii and Tasumi predicted $R_{\text{IR}} > 1$ and $R_{\text{Raman}} < 1$ (*21*).

To obtain a more precise determination of the peptide structure, we utilized the above outlined excitonic coupling algorithm, which explicitly considered all 27 amide I′ modes of Aβ_{1-28}. For the sake of simplicity, we assumed that all on-diagonal force constants of the local modes of the nonterminal peptides were identical. As recently shown by Choi et al., this is approximately justified for extended

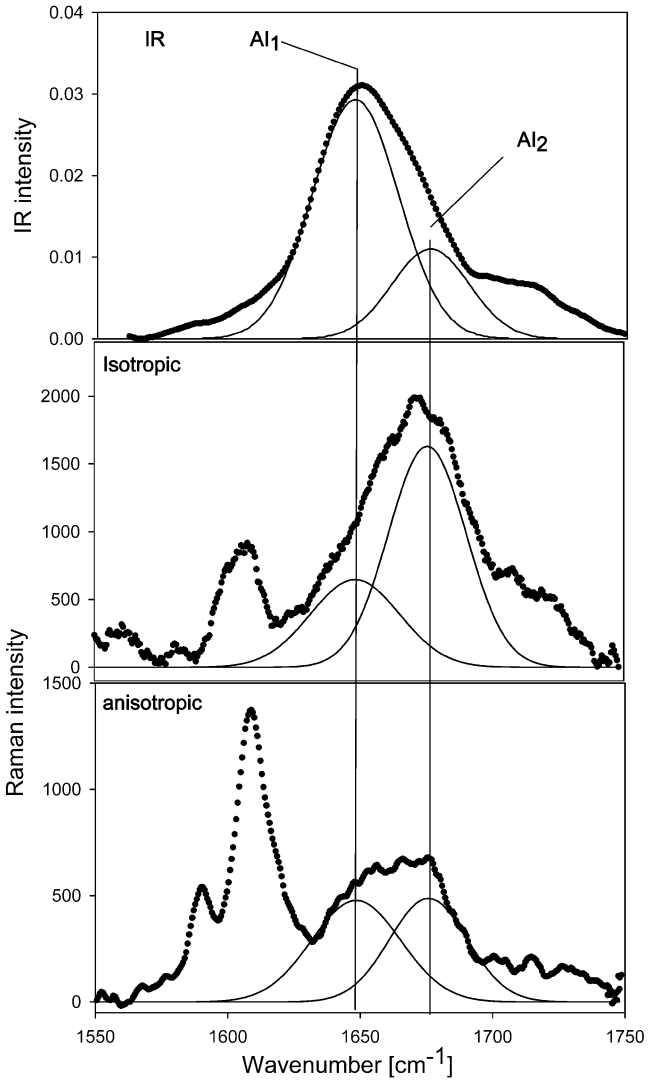

FIGURE 1: FTIR (upper panel) and isotropic and anisotropic Raman spectra ($\lambda_{\text{exc}} = 514$ nm, laser power = 400 mW, and slit width = 100 μm) of Aβ1−28 after TFA removal measured at pD 1.0. The solid lines and the band profiles arise from the fitting procedure described in our previously published articles.

conformations (*22*).[2] Eigenvectors and eigenenergies were calculated by diagonalizing the excitonic Hamiltonian $\hat{H}_{\text{ext}}$, which accounted for nearest-neighbor and second-nearest-neighbor coupling. The coupling energies for the investigated conformations were obtained from our recent studies on tri- and tetrapeptides (nearest neighbor) (*18*, *20*) and by explicitly calculating the transition dipole coupling for second neighbors (*21*). For the wavenumber of the unperturbed modes, we assumed a value of 1657 cm^{-1} for the nonterminal peptide groups as obtained for the central residue of tetra-alanine (*18*). For the N- and C-terminal peptides, we employed wavenumber values of 1648 and 1674 cm^{-1}, respectively, which can be considered as representative values for a variety of earlier investigated tripeptides (*18*, 27). The IR and Raman intensity profiles of amide I′ were then calculated by superimposing the contributions of all 27 delocalized vibrational states. We modeled the individual Raman and IR bands

[2] This paper does not report the local wavenumbers for PPII, but Dr. Cho's group provided us with the results of a calculation for a canonical PPII conformation, which suggest wavenumber variations of ±2 cm^{-1} for the central residues of a hexapeptide.

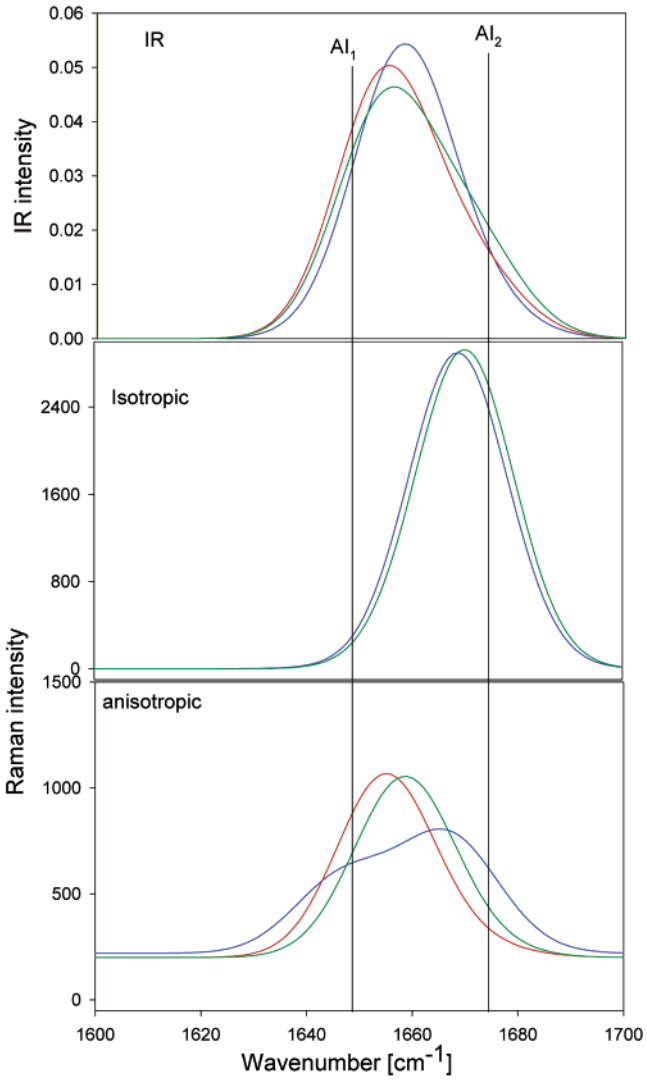

FIGURE 2: Amide I′ band profiles of a 28-residue-containing peptide for different extended conformations, i.e., PPII, $\phi = -75°$, $\psi = 150°$ (blue line), antiparallel β strand, $\phi = -140°$, $\psi = 135°$ (green line), and extended β strand, $\phi = -165°$, $\psi = 150°$ (red line), obtained from a coupled oscillator model described in the text.

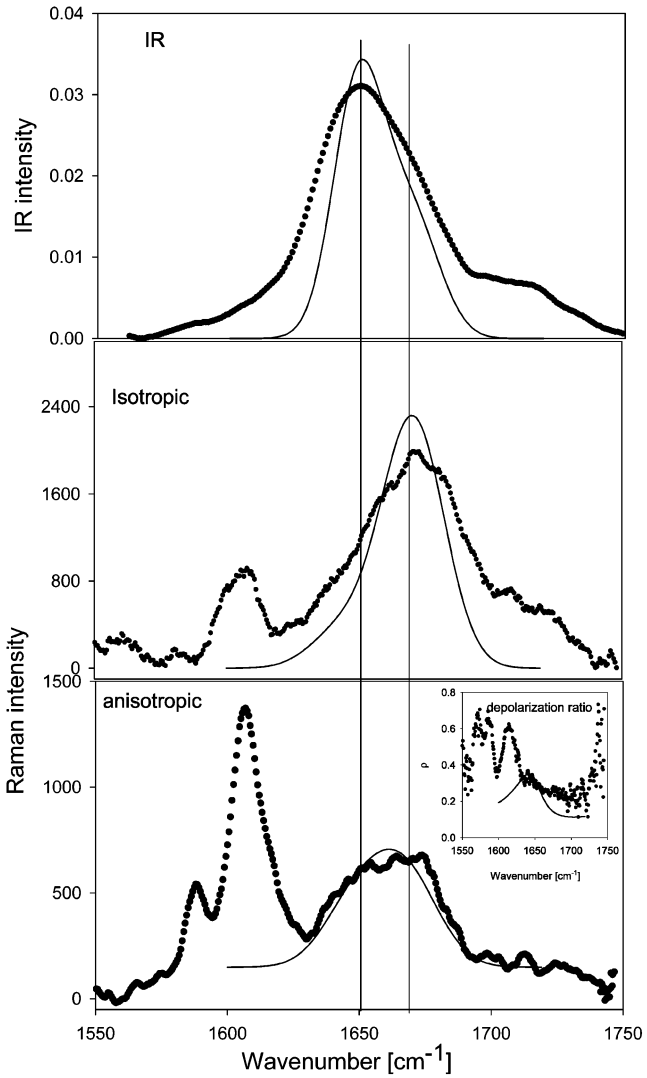

FIGURE 3: Comparison of calculated amide I′ band profiles with the respective experimental spectrum. The calculation (—) was performed by assuming a mixture of local PPII and β-strand conformations as described in the text.

by using Gaussian profiles with a total half-width of 22 cm^{-1}, which is representative of what we obtained for many tripeptides (*20*, *27*).[3] Figure 2 depicts the result of our simulation for three secondary structures, namely, PPII (blue line), an antiparallel sheet β strand (green line), and an extended β strand (red line). For all structures, we reproduced the noncoincidence between the first moments of IR and Raman scattering obtained in the experiment, which is diagnostic of an extended conformation located in the upper-left square of the Ramachandran plot.[4] The three conformers could hardly be distinguished solely by comparing their IR and (isotropic and total) Raman band profiles with the experimental data. The isotropic band profiles of the antiparallel sheet and the extended conformation are identical, because the same coupling constants were used for the simulation. The anisotropic scattering distribution, however, is qualitatively different for β-strand conformations and PPII. The former exhibits a dominant intensity at the AI_1' position, while the latter also depicts a substantial intensity at AI_2'. A comparison between Figures 1 and 2 reveals that the PPII simulation is very similar to the experimentally observed profile. This clearly indicates that a substantial fraction of Aβ_{1-28} exhibits a PPII-like conformation. All simulations do not account for the asymmetry of the isotropic and IR band profile and slightly underestimate the apparent $A - E_1$ difference.[5]

In the next step, we have performed a more realistic simulation in that we utilized results of the recent NMR study of Zagorski et al. (*7*), which suggests that the L^{17}—A^{21} section of Aβ peptides adopts a β-strand conformation. Figure 3 compares the calculated band profiles with the experimental spectra. The agreement with the anisotropic scattering profile is nearly quantitative. The calculated IR and isotropic Raman profiles show the asymmetry depicted by the experimental data. The $A - E_1$ difference is well-reproduced. The

[3] We thus neglected the much smaller Lorentzian contribution to what is normally a Voigtian profile.

[4] As a test of our program, we also calculated the spectra for a right-handed α helix. As expected, we found a coincidence of isotropic Raman and IR absorption.

[5] For the sake of convenience, we continue using this notation even though a two-mode approach is certainly an oversimplification.

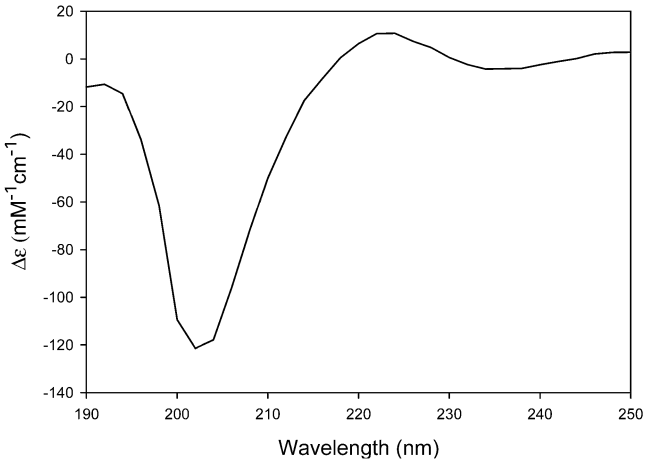

FIGURE 4: ECD spectrum of 1 mM acidic Aβ_{1-28} at room temperature.

simulation also accounts for the depolarization ratio in the E_1-band region (inset in the lower panel of Figure 3). All this suggests, considering a mixture of PPII and β strand, is a more realistic structural model. The still existing discrepancies between the theory and experiment are likely to reflect the inadequacy of our assumption that the Raman tensors and transition dipole moments of all peptide groups are identical. A more refined model based on the IR and Raman measurements of XA and AX peptides is currently underway in our laboratory. However, the present level of theory is sufficient to provide substantial evidence for the notion that PPII is the predominant conformation of monomeric Aβ_{1-28}. This conclusion is consistent with the increasingly accepted interpretation of the ECD spectrum of the peptide shown in Figure 4 (*28*, 29).

Additionally, we performed several simulations for other possible conformations assignable to the upper-left quadrant of the Ramachandran plot to explore the possibility that the observed spectra reflect a mixture of different conformers including PPII as suggested by the classical random-coil model (*30*, *31*, 32). Thus, we found that the experimentally obtained anisotropic scattering distribution is reproduced only in a very restricted range of dihedral angles around the classical PPII coordinate. Moreover, it became apparent that many conformations with ϕ angles between $-60°$ and $-140°$ give rise to a significantly reduced $A - E_1$ difference. Hence, a mixture of multiple conformations would cause a substantial broadening of the spectra and a reduced noncoincidence between IR and isotropic Raman scattering, which would make the spectra much less characteristic as experimentally observed.

In general, the amyloidogenesis is frequently described in terms of an α-helix to β-sheet transition (*33*, 34, 35) involving a partially unfolded intermediate. Barron and co-workers provided evidence that such intermediates may involve a substantial fraction of PPII (*11*, *12*). For amyloid peptides, the situation is slightly different. The helical conformation can only exist in a supportive environment provided by reagents such as TFE and/or by charged membrane surfaces, which can be mimicked by sodium dodecyl sulfate or dodecylphoshocholine micelles (*8*, 36). In a pure aqueous solution, the peptide is considered to be either monomeric random coil or aggregated (*7*). The former conformation could be related to the folding intermediate observed for amyloid-forming proteins. Our observation of a substantial PPII fraction fits into that picture and is in line with the hypothesis that PPII is the killer conformation as suggested by Blanch et al. (*11*). In more specific terms, the present result and those of Barron and co-workers (*11*, *12*) suggest that it is the high stability of PPII with respect to an α-helical conformation and a classical random-coil state that gives rise to the high propensity for aggregation. As pointed out by Syme et al. (*12*), a real random-coil conformation would lead to amorphous aggregates rather than to ordered fibrils. The admixture of structurally well-defined hydrophobic segments L17−F20 and I31−V36 (*7*) significantly increase the propensity for β-sheet aggregation (*37*, 38). We like to emphasize, however, that PPII formation cannot be considered as a necessary condition for the formation of amyloid plaques as demonstrated by the absence of any PPII-like intermediate in the aggregation process of the prion scrapie fragment PrP$^{94-223}$ (*35*).

Besides exploring the structure of Aβ_{1-28}, this paper, for the first time, reports a detailed and quantitative analysis of vibrational spectra, which demonstrates the combined use of IR and isotropic and anisotropic Raman spectra for the structural analysis of peptides. Generally, researchers confine themselves to solely using FTIR on a much less-quantitative level. As an exception from this rule, Carey, Anderson, and co-workers recently reported a visible Raman study on α synuclein (*39*). For the respective aqueous solution of the protein, they obtained an asymmetric Raman band profile at 1674 cm^{-1}, which is very similar to the isotropic Raman band in Figure 1. They somewhat tentatively assigned it to PPII, guided by the results of Barron and co-workers (*12*). While we agree with their assignment, we like to emphasize that an interpretation just based on unpolarized Raman is problematic. This paper shows that polarized Raman measurements provide much more useful information. Additionally, it is somewhat problematic to decompose asymmetric bands into different Gaussian profiles and assign them to different secondary structures. As demonstrated in this paper, excitonic coupling yields a delocalization of amide I states and thus an asymmetric band shape. We will deal with this issue in more detail in a separate paper.

ACKNOWLEDGMENT

We are indebted to Dr. Michael Zagorski for his advise concerning the handling of Aβ_{1-28}. We also thank Wasfi Al-Azzam for his help regarding the Aβ_{1-28} dialysis procedure. Moreover, we thank Tom Measey and Andrew Hagarman for carefully checking the style and language of the paper. R.S.S. thanks Dr. Minhaeng Cho for fruitful discussion about the physical determinants of the amide I mode in polypeptides and for providing us results about the variation of the local amide I wavenumber in a PPII conformation.

REFERENCES

1. Kang, J., Lemaire, H. G., Unterbeck, A., Salbaum, J. M., Masters, C. L., Grzeschick, K. H., Multhaup, G., Beyreuther, K., and Mueller-Hill, B. (1987) The precursor of Alzheimer's disease amyloid A4 protein resembles a cell-surface receptor, *Nature 325*, 733−736.
2. Ishiura, S. (1991) Proteolytic cleavage of the Alzheimer's disease amyloid A4 precursor protein, *J. Neurochem. 56*, 363−369.
3. Mueller-Hill, B., and Beyreuther, K. (1989) Molecular biology of Alzheimer's disease, *Annu. Rev. Biochem. 58*, 287−307.

4. Fraser, P. E., Nguyen, J. T., Surewicz, W. K., and Kirschner, D. A. (1991) pH-dependent structural transitions of Alzheimer amyloid peptides, *Biophys. J. 60*, 1190−1201.
5. Golde, T. E, Estus, S., Younkin, L. H., Selkoe, D. J., and Younkin, S. G. (1992) Processing of the amyloid protein precursor to potentially amyloidogenic derivatives, *Science 255*, 728−730.
6. Hilbich, C., Kisters-Woike, B., Reed, J., Masters, C. L., and Beyreuther, K. (1991) Aggregation and secondary structure of synthetic amyloid β A4 peptides of Alzheimer's disease, *J. Mol. Biol. 218*, 149−163.
7. Hou, L., Shao, H., Zhang, Y., Li, H., Menomn, M. K., Neuhaus, E. B., Brewer, J. M., Byeon, I.-J., Ray, D. G, Vitek, M. P., Iwashita, T., Makula, R. A., Przybala, A. B., and Zagorski, M. G. (2004) Solution NMR studies of the Aβ(1−40) and Aβ(1−42) peptides establish that the Met35 oxidation state affects the mechanism of amyloid formation, *J. Am. Chem. Soc. 126*, 992.
8. Ma, K., Clancy, E. L., Zhang, Y., Ray, D. G., Wollenberg, K., and Zagorski, M. G. (1999) Residue-Specific pK_a Measurements of the β-Peptide and Mechanism of pH-Induced Amyloid Formation, *J. Am. Chem. Soc. 121*, 8698−8706.
9. Jarvet, J., Damberg, P., Danielsson, J., Johansson, I., Eriksson, L. E. G., and Gräslund, A. (2003) A left-handed 3(1) helical conformation in the Alzheimer Aβ(12−28) peptide, *FEBS Lett. 555*, 371−374.
10. Huang, T. H., Fraser, P. E., and Chakrabattay, A. (1997) Fibrillogenesis of Alzheimer Aβ peptides studied by fluorescence energy transfer, *J. Mol. Biol. 269*, 214−224.
11. Blanch, E. W., Morozova-Roche, L. A., Cochran, D. A. E., Doig, A. J., Hecht, L., and Barron, L. D. (2000) Is polyproline II helix the killer conformation? A Raman optical activity study of the amyloidogenic prefibrillar intermediate of human lysozyme, *J. Mol. Biol. 301*, 553−556.
12. Syme, C. D., Blanch, E. W., Holt, C., Jakes, R., Goedert, M., Hecht, L., and Barron, L. D. (2002) A Raman optical activity study of rheomorphism in caseins, synucleins, and τ. New insight into the structure and behaviour of natively unfolded proteins, *Eur. J. Biochem. 269*, 148−156.
13. Chiti, F., Stefani, M., Taddei, N., Ramponi, G., and Dobson, C. M. (2003) Rationalization of the effects of mutations on peptide and protein aggregation rates, *Nature 424*, 805.
14. Talafous, J., Marcinowski, K. J., Klopman, G., and Zagorski, M. G. (1994) Solution structure of residues 1−28 of the amyloid β-peptide, *Biochemistry 33*, 7788.
15. Kirschner, D. A., Inouye, H., Duffy, L. K., Sinclair, A., Lind, M., and Selkoe, D. J. (1987) Synthetic peptide homologous to β protein from Alzheimer disease forms amyloid-like fibrils in vitro, *Proc. Natl. Acad. Sci. U.S.A. 84*, 6953−6957.
16. Gorevic, P. D., Castano, E. M., Sarma, R., and Frangione, B. (1987) Ten to fourteen residue peptides of Alzheimer's disease protein are sufficient for amyloid fibril formation and its characteristic X-ray diffraction pattern, *Biochem. Biophys. Res. Commun. 147*, 854−862.
17. Fraser, P. E., McLachlan, D. R., Surewicz, W. K., Mizzen, C. A., Snow, A. D., Nguyen, J. T., and Kirschner, D. A. (1994) Conformation and fibrillogenesis of Alzheimer Aβ peptides with selected substitution of charged residues, *J. Mol. Biol. 244*, 64−73.
18. Schweitzer-Stenner, R., Eker, F., Griebenow, K., Cao, X., Nafie, L. (2004) The conformation of tetraalanine in water determined by polarized Raman, FT-IR, and VCD spectroscopy, *J. Am. Chem. Soc. 126*, 2768.
19. Schweitzer-Stenner, R. (2002) Dihedral angles of tripeptides in solution directly determined by polarized Raman and FTIR spectroscopy, *Biophys. J. 83*, 523.
20. Eker, F., Cao, X., Nafie, L., and Schweitzer-Stenner, R. (2002) Tripeptides adopt stable structures in water. A combined polarized visible Raman, FTIR, and VCD spectroscopy study, *J. Am. Chem. Soc. 124*, 14330−14341.
21. Torii, H., and Tasumi, M. (1998) Ab initio molecular orbital study of the amide I vibrational interactions between the peptide groups in di- and tripeptides and considerations on the conformation of the extended helix, *J. Raman Spectrosc. 29*, 81−86.
22. Choi, S.-J., Ham, S., and Cho, M. (2003) Local Amide I Mode Frequencies and Coupling Constants in Polypeptides, *J. Phys. Chem. B 107*, 9132−9138.
23. Schweitzer-Stenner, R., Eker, F., Perez, A., Griebenow, K., Cao, X., and Nafie, L. (2003) The structure of tri-proline in water probed by polarized Raman, Fourier transform infrared, vibrational circular dichroism, and electric ultraviolet circular dichroism spectroscopy, *Biopolymers 71*, 558−568.
24. Glasoe, P. K., and Long, F. A. (1960) Use of glass electrodes to measure acidities in deuterium oxide, *J. Phys. Chem*. 64, 188−193.
25. Jao, S.-c., Ma, K., Talafous, J., Orlando, R., and Zagorski, M. G. (1997) Trifluoroacetic Acid Pretreatment Reproducibly Disaggregates the Amyloid β Peptide, *Amyloid 4*, 24−252.
26. Jentzen, W., Unger, E., Karvounis, G., Shelnutt, J. A., Dreybrodt, W., and Schweitzer-Stenner, R. (1996) Conformational Properties of Nickel(II) Octaethylporphyrin in Solution. 1. Resonance Excitation Profiles and Temperature Dependence of Structure-Sensitive Raman Lines, *J. Phys. Chem. 100*, 14184−14191.
27. Eker, F., Griebenow, K., Cao, X., Nafie, L., and Schweitzer-Stenner, R. (2004) Tripeptides with ionizable side chains adopt a perturbed polyproline II structure in water, *Biochemistry 43*, 613−621.
28. Shi, Z., Woody, R. W., and Kallenbach, N. R. (2002) Is polyproline II a major backbone conformation in unfolded proteins? *Adv. Protein Chem. 62*, 163−2410.
29. Eker, F., Griebenow, K., and Schweitzer-Stenner, R. (2003) Stable conformations of tripeptides in aqueous solution studied by UV circular dichroism spectroscopy, *J. Am. Chem. Soc. 175*, 8178−8185.
30. Brant, D. A., and Flory, P. J. J. (1965) The Configuration of Random Polypeptide Chains. II. Theory, *J. Am. Chem. Soc. 87*, 2791.
31. Tanford, C. (1968) Protein denaturation, *Adv. Protein Chem. 23*, 121−282.
32. Zimmermann, S. S., Pottle, M. S., Némethy, G., and Scheraga, H. A. (1977) Conformational Analysis of the 20 Naturally Occurring Amino Acid Residues Using ECEPP, *Macromolecules 10*, 1−9.
33. Prusiner, S. B. (1991) Molecular biology of Prion diseases, *Science 252*, 1515−1521.
34. Mihara, H., Takahashi, Y., and Ueno, A. (1998) Design of peptides undergoing self-catalytic α-to-β transition and amyloidogenesis, *Biopolymers 47*, 83.
35. McColl, I. H., Blanch, E. W., Gill, A. C., Rhie, A. G. O., Ritchie, M. A., Hecht, L., Nielsen, K., and Barron, L. D. (2003) A new perspective on β-sheet structures using vibrational Raman optical activity: From poly(L-lysine) to the prion protein, *J. Am. Chem. Soc. 125*, 10019.
36. Barrow, C. J., and Zagorski, M. Z. (1991) Solution structures of β peptide and its constituent fragments: relation to amyloid deposition, *Science 253*, 179−182.
37. Esler, W. P., Stimson, E. R., Ghilardi, J. R., Lu, Y.-A., Felix, A. M., Vinters, H. V., Mantyh, P. W., Lee, J. P., and Maggio, J. E. (1996) Point substitution in the central hydrophobic cluster of a human β-amyloid congener disrupts peptide folding and abolishes plaque competence, *Biochemistry 35*, 13914.
38. Mansfield, S. L., Gotch, A. J., Harms, G. S., Johnson, C. K., and Larive, C. K. (1999) Complementary Analysis of Peptide Aggregation by NMR and Time-Resolved Laser Spectroscopy, *J. Phys. Chem. B 103*, 2262−2269.
39. Maiti, N., Apetri, M. M., Zagorski, M. G., Carey, P. R., and Anderson, V. E. (2004) Raman spectroscopic characterization of secondary structure in natively unfolded proteins: α-Synuclein, *J. Am. Chem. Soc. 126*, 2399.

BI049542+